Published in final edited form as:
Circ Res. 2014 March 14; 114(6): 982–992. doi:10.1161/CIRCRESAHA.114.302711.

A Role for Myosin V Motor Proteins in the Selective Delivery of Kv Channel Isoforms to the Membrane Surface of Cardiac Myocytes

Sarah M. Schumacher-Bass[1], **Eileen D. Vesely**[1], **Lian Zhang**[1], **Katherine E. Ryland**[1], **Dyke P. McEwen**[2], **Priscilla J. Chan**[3], **Chad R. Frasier**[1], **Jeremy C. McIntyre**[1], **Robin M. Shaw**[4], and **Jeffrey R. Martens**[1]

[1]Department of Pharmacology, University of Michigan, Ann Arbor, MI 48109

[2]Essen BioScience, Ann Arbor, MI 48108

[3]University of California, San Francisco, CA 951483

[4]Cedars-Sinai Medical Center, Los Angeles, CA 90048

Abstract

Rationale—Kv1.5 (KCNA5) mediates the I_{Kur} current that controls atrial action potential duration. Given its atrial-specific expression and alterations in human atrial fibrillation (AF), Kv1.5 has emerged as a promising target for the treatment of AF. A necessary step in the development of novel agents that selectively modulate trafficking pathways is the identification of the cellular machinery controlling Kv1.5 surface density, of which little is yet known.

Objective—To investigate the role of the unconventional myosin V (MYO5A and MYO5B) motors in determining the cell surface density of Kv1.5.

Methods and Results—Western Blot analysis showed MYO5A and MYO5B expression in the heart, while disruption of endogenous motors selectively reduced I_{Kur} current in adult rat cardiomyocytes. Dominant negative constructs and shRNA silencing demonstrated a role for MYO5A and MYO5B in the surface trafficking of Kv1.5 and Connexin-43 (Cx43), but not hERG (KCNH2). Live-cell imaging of Kv1.5-GFP and retrospective labeling of phalloidin demonstrated motility of Kv1.5 vesicles on actin tracts. MYO5A participated in anterograde trafficking, while MYO5B regulated post-endocytic recycling. Over-expression of mutant motors revealed a selective role for Rab11 in coupling MYO5B to Kv1.5 recycling.

Conclusions—MYO5A and MYO5B control functionally distinct steps in the surface trafficking of Kv1.5. These isoform-specific trafficking pathways determine Kv1.5-encoded I_{Kur} in myocytes to regulate repolarizing current, and consequently, cardiac excitability. Therapeutic strategies that manipulate Kv1.5 selective trafficking pathways may prove useful in the treatment of arrhythmias.

Address correspondence to: Dr. Jeffrey R. Martens, University of Florida, Department of Pharmacology and Therapeutics, PO Box 100267, 1200 Newell Dr, Gainesville, FL 32610, Tel: 352-294-5352, Fax: 352-392-3558, martensj@ufl.edu.
S.M.S-B. and E.D.V. contributed equally to this study.

DISCLOSURES
None.

Keywords

Kv1.5; heart; trafficking; myosin motors; connexin-43; K channel; arrhythmia

INTRODUCTION

Atrial fibrillation (AF) is the most common cardiac arrhythmia and represents a significant health risk to the population. Therapy for AF seeks to restore normal sinus rhythm through pharmacologic cardioversion[1–4]. Lack of ion channel selectivity and overlap in ion channel expression in the atria and ventricles however, underlies the nonspecific ventricular side effects of current pharmacological agents[5, 6]. Therefore, strategies for the treatment of AF, targeting ion channels selectively expressed in the human atria, may offer a therapeutic advantage.

In the human atria, the voltage-gated potassium channel Kv1.5 underlies a major repolarizing current, I_{Kur}. The role of I_{Kur} in the control of action potential duration and atrial refractory period highlights its importance in atrial excitability and recognition as a major target for the treatment of AF[7–10]. Further, loss-of-function mutation in KCNA5 has been shown to cause AF in humans[8].

Despite the emergence of multiple new antiarrhythmic drugs that target I_{Kur}, effective cardioversion with clinical efficacy and safety has yet to be achieved[11]. Drug-induced internalization of Kv1.5 in atrial myocytes,[12] suggests a novel therapeutic avenue for the acute termination of AF through manipulation of ion channel trafficking, which may avoid the non-selectivity associated with pore-block of potassium channels. One limiting factor shared by these approaches is that during the transition from paroxysmal to permanent AF, there is a marked reduction in I_{Kur}, accompanied by a decrease in Kv1.5 protein expression[10]. The electrical remodeling, and decreased Kv1.5 sensitivity to antiarrhythmic compounds during chronic AF[13], highlights the need for further understanding of the molecular mechanisms regulating Kv1.5 surface density.

Chronic AF is characterized by both electrical and structural remodeling that includes cytoskeletal rearrangement during the progression of this disease[14–17]. Given that protein trafficking is thought to occur through a cooperation of long-range trafficking, along microtubules, and short-range movement, along actin filaments in the periphery, such a disruption could significantly abrogate cell surface levels and localization of cardiovascular ion channels[18–22]. There is evidence for a role of the microtubule and actin cytoskeleton in the regulation of Kv1.5 current[23–33] linking the disruption of the actin cytoskeleton and Kv1.5 trafficking to the onset of AF[34]. Further, this disruption of Kv1.5 trafficking was shown to cause arrhythmias and sudden-arrhythmic death in mice.

In general the molecular machinery identities of the molecular motors and adaptors regulating ion channel trafficking in the cardiovascular system remain unknown. Here we report, for the first time, the role of the unconventional myosin motors, MYO5A and MYO5B in determining the cell surface level of Kv1.5, in cardiomyocytes, and show a specific role for MYO5B coupling to Rab11 to control channel recycling.

METHODS

See Online supplement for detailed methods.

Immunocytochemistry

Immunocytochemistry was performed and all images were collected, quantified, and analyzed as reported earlier[26].

Electrophysiology

Whole-cell voltage clamp experiments were performed on adult rat ventricular myocytes and HL-1 cells expressing Kv1.5-GFP at room temperature as described previously[28].

Ventricular myocyte isolation

Adult rat and mouse neonatal ventricular myocytes were isolated using previously established protocols[28, 35].

Quantification of Cx43 gap junction plaque density

To quantify Cx43 expression at cell-cell borders, maximum intensity projections of 10 μm confocal z-stacks were generated for N-cadherin (to identify borders) and Cx43. We then implemented a MATLAB routine, which generates 10-micron fluorescence intensity profiles bisecting traced cell-cell borders. This routine is freely available upon request[35, 36].

RESULTS

Disruption of MYO5A or MYO5B inhibits I_{Kur} current in adult rat myocytes

Kv1.5 trafficking, surface expression, and function depends upon interaction with the actin cytoskeleton,[27, 29] as well interactions with PDZ domains of PSD-95, SAP97, and alpha-actinin-2[29–32, 37]. While these data indicate a connection of the actin cytoskeleton with Kv1.5 localization, the direct mechanistic link between actin filaments and trafficking of Kv1.5 to the plasma membrane is unknown. Two candidate unconventional myosin motors, MYO5A and MYO5B, transport cargo along actin filaments and play a critical role in normal function and excitability in various cell types[18], however little is known regarding their role in the excitability and function of cardiomyocytes. Myo5a and Myo5b mRNA are detected in the heart,[38, 39] however protein presence is unknown. Using specific antibodies, endogenous MYO5A and MYO5B was detected via western blot in protein lysates from both rat heart and HL-1 atrial myocytes (Figure 1A).

To address the importance of MYO5A and MYO5B in determining Kv1.5 current levels in native myocytes, we developed replication-deficient adenoviral vectors coding for only their cargo-binding domains (globular tail domain). These constructs act as dominant-negatives (DN) by sequestering cargo in the presence of endogenous motor and discriminate between their functional roles. Although Kv1.5 is atrial-specific in humans, in rodents it is expressed in both atria and ventricles. To study channel trafficking in native myocytes we used acutely dissociated adult rat ventricular myocytes. Ectopic expression was confirmed by visualization of RFP fused to both Myo5-DN isoforms (Figure 1B). Isolation of I_{Kur} from

myocytes was achieved by sequential whole cell voltage clamp traces using a previously described protocol[28] (Figure 1C). Briefly I_{ss} was subtracted from the previous trace (I_{Kur} + I_{ss}) to measure I_{Kur}. Expression of Myo5aDN or Myo5bDN resulted in a significant decrease in I_{Kur} in acutely dissociated ventricular myocytes 24 hours post-transduction (53 ± 8% and 58 ± 6%, $n \geq 7$ myocytes; $p < 0.05$ and 0.01, respectively) (Figure 1D). Using a second selective Kv1.5 inhibitor, DPO-1, we confirmed that MYO5aDN and Myo5bDN significantly reduced Kv1.5 current density (Figure 1D). Importantly, Myo5DN transduction did not alter I_{ss} in myocytes, showing specificity of this effect and a lack of generalized toxicity due to adenoviral transduction. Together these data indicate a potential role for MYO5a and MYO5B in regulating Kv1.5-encoded I_{Kur} in cardiomyocytes.

MYO5a and MYO5B control steady-state cell surface levels of Kv1.5 and Cx43

The selective decrease in I_{Kur} could result from alterations in channel conductance or in the cell surface density of Kv1.5 channel protein. To investigate the underlying mechanism, we used HL-1 immortalized mouse atrial myocytes expressing an extracellular GFP epitope-tagged Kv1.5 (Kv1.5-GFP) that mimics wild-type channel function[12, 26]. In agreement with our native myocyte data, co-expression with Myo5aDN or Myo5bDN resulted in a significant decrease in Kv1.5 current density (64 ± 29% and 34 ± 28% decrease in current density, respectively; $n \geq 5$; $p < 0.05$) (Figure 2A). This decrease in current density was greater in the presence of both myosin-V DN isoforms, resulting in a 92 ± 4% decrease in Kv1.5 current. To determine whether the decrease in current density was the result of a reduction in cell surface trafficking, we measured the effect of co-expression of Myo5aDN or Myo5bDN on steady-state cell surface levels of Kv1.5-GFP. Co-expression of Myo5aDN or Myo5bDN with Kv1.5-GFP resulted in a 47 ± 2% and 32 ± 3% decrease in surface channel, respectively ($n \geq 73$, $p < 0.001$) (Figure 2B, Online Figure IA). Co-expression with both Myo5DN constructs further reduced cell surface Kv1.5-GFP by 63 ± 2%. In contrast, co-expression with either Myo5DN construct did not alter the cell surface levels of extracellular-tagged hERG-GFP ($n \geq 27$) (Figure 2C, Online Figure IB). Interestingly, our data revealed no change in Iss current, suggesting that hERG, and other channels that make up the Iss current, are unaffected by the disruption of these myosin motors, further suggesting myosin-V motors act selectively to traffic Kv channel isoforms.

As an alternative, complimentary approach for testing the role of myosin-V in regulating Kv1.5 surface density, we used gene silencing with short hairpin RNA (shRNA) constructs targeted specifically against endogenous Myo5a and Myo5b. To control for efficiency, the shRNA constructs were expressed using lentiviral infection. These shRNA constructs effectively reduced the expression of recombinant MYO5A and MYO5B in infected HL-1 myocytes (Online Figure IIB, C). No decrease in expression was observed when HL-1 cells were transfected with Myo5a or Myo5b carrying silent mutations (shRNA resistant). With the effectiveness and specificity of the myosin gene silencing established, we measured the effects on Kv1.5-GFP surface density. Infection of cells with Myo5a or Myo5b shRNA, but not the scrambled control, significantly decreased Kv1.5-GFP surface levels (59 ± 2% and 51 ± 2% respectively; $n \geq 93$; $p < 0.001$) (Figure 2D, Online Figure IIA). Together these two methods strongly implicate MYO5A and MYO5B mediated trafficking in determining the steady-state cell surface levels and current density of Kv1.5.

Importantly, we investigated if myosin-V control of Kv1.5 surface expression is conserved in native cardiomyocytes by analyzing cell surface localization of ectopically expressed Kv1.5-GFP and Kv1.5 specific current density in isolated rat ventricular myocytes. Consistent with surface expression data using immortalized HL-1 cells, co-expression of Kv1.5-GFP with either Myo5aDN, or Myo5bDN, resulted in a significant decrease in Kv1.5-GFP cell surface levels compared to mCherry control ($n \geq 28$, $p < 0.001$) (Figure 3A and 3B). Under whole cell voltage clamp, co-infection of Kv1.5-GFP with either Myo5aDN or Myo5bDN, significantly decreased Kv1.5 specific current density ($n \geq 6$, $p < 0.05$) (Figure 3D). Comparison of Kv1.5 channel proteins at the surface of live cells (Figure 3A) and that of permeabilized cells (Figure 3C) revealed that the observed decreases in both the cell surface density and the current density of Kv1.5 were due to a population of Kv1.5 channels that was restricted to the interior of the cell. While little or no Kv1.5-GFP surface expression was detected in the presence of Myo5aDN and Myo5bDN, the permeabilized cells show an accumulation of channel just under the surface at the cell border, particularly in the presence of Myo5aDN.

While our data indicate that MYO5A and MYO5B show selectivity for Kv channel isoforms, we tested whether they play a role in the regulation of other proteins found at the cell-cell border. Deletion of connexin-43 (Cx43) in human atrial tissue has been associated with trafficking defects and the onset of AF, [36, 40] therefore, we investigated the trafficking and surface localization of CX43 at the gap junctions found at cell-cell borders by monitoring its distance from the cell border of neonatal mouse ventricular myocytes. Myocytes were transduced with either adenoviral LacZ, or Myo5aDN, or Myo5bDN, in the presence of Brefeldin A (BFA), to inhibit the anterograde movement of the Cx43 protein to the plasma membrane. After 12 h of BFA treatment the majority of Cx43 in the cytoplasm and at cell-cell borders is degraded and new Cx43 is localized in the ER, appearing diffuse throughout the cell interior. This technique allows for enrichment of Cx43 early in the vesicular transport pathway and, with washout, to subsequently study anterograde transport in the absence of confounding signal from Cx43 already at the cell surface. Two hours post-washout, Cx43 is apparent in perinuclear Golgi apparatus, and at four hours, the majority of Cx43 enriched in the ER will have had sufficient time to traverse the vesicular transport pathway and have undergone delivery to the cell cortex[36]. Quantification of Cx43 expression at cell-cell borders 4 h post-washout (Figure 4C) was achieved using a MATLAB routine to generate 10 μm fluorescence intensity profiles perpendicular to, and bisecting traced cell-cell borders[41]. The wider intensity profile (Figure 4C, red) of Cx43 distribution in the presence of the Myo5aDN indicates accumulation of Cx43 in subcortical non-border regions. These data are consistent with Kv1.5 channel data in the presence of the Myo5aDN and Myo5bDN, and suggests that, the MYO5A motor is not specific for the regulation of Kv1.5 channel proteins.

MYO5A and MYO5B regulate the intracellular trafficking of Kv1.5 along actin filaments at the periphery of the myocyte

To investigate whether the decrease in Kv1.5-GFP surface localization was due to a loss of channel trafficking on actin filaments, we first confirmed a role for the intact actin cytoskeleton in modulating surface density of the channel. Acute treatment with

cytochalasin D, resulted in a time-dependent decrease in surface Kv1.5 that was significant after one hour and culminated in a 56 ± 6% decrease after 6hr ($n \geq 85$; $p < 0.001$) (Figure 5A, Online Figure III). To directly demonstrate the motility of Kv1.5-GFP vesicles on actin filaments, we performed live-cell, time-lapse imaging, 16–20 hours post-transfection, followed by retrospective immunofluorescence labeling and static imaging of the actin cytoskeleton (Figure 5B). Kv1.5-GFP labeled vesicles were clearly visualized moving on phalloidin-labeled actin tracts at the periphery. Retrospective labeling of both phalloidin and tubulin showed Kv1.5-GFP vesicles moving in the anterograde direction on microtubules and transitioning to actin filaments at the myocyte edge. To measure the ensemble characteristics of Kv1.5-GFP motility, we used a standard deviation (SD) map to sum all motility events of a time series into one image[23]. An overlay of the SD map of Kv1.5-GFP with a retrospectively labeled image of the actin cytoskeleton clearly demonstrates movement of Kv1.5-GFP-containing vesicles on linear tracts marked by phalloidin (Figure 5C). This processivity of Kv1.5-GFP-containing vesicles on actin is lost in the presence of Myo5aDN or Myo5bDN. Quantification of trafficking events revealed that co-expression with either myosin-V DN construct significantly reduced both the average distance traveled and the average net velocity of Kv1.5-GFP-contatining vesicles along actin filaments (Figure 5D). Kv1.5-GFP alone, exhibited an average travel distance of 0.8 μm and a velocity of approximately 0.4 μm/s (400 nm/s) consistent with previous literature,[42–46] whereas co-expression with Myo5aDN or Myo5bDN resulted in a 30 ± 1% and 33 ± 2% decrease in distance and velocity, respectively. These combined results demonstrate that MYO5A and MYO5B contribute to the actin-based transport of Kv1.5 vesicles in HL-1 myocytes.

Myosin-V Isoforms act at distinct steps in the Kv1.5 trafficking pathway

The additive nature of the MYO5A- and MYO5B-mediated decrease in current density and surface levels suggested that these two myosin-V isoforms might function in different steps in the trafficking pathway of Kv1.5 (Figure 2A, 2B). Therefore, we next tested whether there was a functional distinction between MYO5A and MYO5B in the intracellular trafficking of Kv1.5 in the heart. Previously, we demonstrated acute inhibition of constitutive endocytosis of Kv1.5 with Dynasore, a small molecule inhibitor of dynamin (dyn)[12]. Disruption of dyn-mediated endocytosis permits investigation of the role of MYO5A and MYO5B in the pre- and post-endocytic trafficking of Kv1.5. Introduction of a single point mutation, S61D, in dyn (dynS61D) significantly reduces GTP hydrolysis efficiency, resulting in a DN form for chronic inhibition of constitutive endocytosis[47]. Expression of dynS61D significantly increased steady-state cell surface Kv1.5-GFP, whereas expression of wild-type dyn resulted in decreased surface Kv1.5-GFP (Online Figure IVA, B). More importantly, while co-expression with dyn significantly increased Kv1.5-GFP internalization, internalization decreased in the presence of dynS61D (Online Figure IVC, D).

We then utilized dynS61D to elucidate whether MYO5A and MYO5B were acting upstream or downstream of channel endocytosis. DynS61D blocked the Myo5bDN-mediated decrease in steady-state cell surface Kv1.5-GFP ($n \geq 59$; $p < 0.001$), but did not affect the decrease in surface Kv1.5-GFP mediated by Myo5aDN (Figure 6A, Online Figure VA, B). These data indicate that MYO5A acts in the pre-endocytic and MYO5B in the post-endocytic

trafficking of Kv1.5. To investigate their role in anterograde delivery of Kv1.5-GFP to the plasma membrane we measured the effect of the myosin-V DNs at 6hrs of channel expression, when the majority of surface Kv1.5-GFP is derived from anterograde delivery of newly synthesized channel. 6hrs post-transfection MYO5aDN but not Myo5bDN significantly reduced cell surface levels of Kv1.5-GFP (41 ± 4.7%, n ≥ 25) (Figure 6B, Online Figure VIA, B). These data are consistent with the regulation Kv1.5 and Cx43 by MYO5A motors in native myocyte studies (Figure 3 and Figure 4).

To investigate the role of MYO5B in the post-endocytic recycling of Kv1.5 to the myocyte membrane, we measured constitutive recycling of Kv1.5-GFP in the presence of the Myo5aDN or Myo5bDN, using a live-cell recycling assay (See Online Methods). Myo5bDN, but not Myo5aDN, significantly reduced constitutive channel recycling (73 ± 2.8%, n ≥ 74) (Figure 6C, Online Figure VIIA). Furthermore, this loss of channel recycling through MYO5B led to a partial overlap of Kv1.5-GFP in Rab11 positive perinuclear endosomes in the presence of Myo5bDN. (Figure 6D, Online Figure VIIB). Rab11 is associated with recycling proteins to the cell surface[48, 49] and it has been previously demonstrated that steady-state surface levels of Kv1.5 decrease when co-expressed with GDP-locked Rab mutants[26]. These data demonstrate that MYO5A and MYO5B act in two distinct steps in the cell surface trafficking of Kv1.5.

MYO5B-mediated channel recycling is dependent upon coupling to Rab11

MYO5A has previously been shown to bind Rab11, and to be involved in vesicle trafficking[50]. MYO5B is less well studied; however it is known to interact with Rab11 and is essential to recycling of cAMP activated chloride channels[51] and AMPA receptors[52] from recycling endosomes. Previously, we demonstrated a role of Rab11, but not Rab8, in the post-endocytic recycling of Kv1.5 in atrial myocytes.[26] To test whether Rab11 couples Kv1.5-containing vesicles with MYO5B during channel recycling, we utilized recently characterized mutations in MYO5B that disassociate the motor from Rab-GTPases[53]. Co-expression of Kv1.5 with the Rab11 binding-deficient MYO5B Y1684E/Q1718R (Myo5bYE/QR) resulted in a 52 ± 1.5% decrease in channel surface density (n ≥ 74, $p < 0.001$) (Figure 7A, Online Figure VIIIA). In contrast, co-expression with the Rab8 binding-deficient MYO5B mutant Q1296L/Y1303C (Myo5bQL/YC) did not alter the steady-state cell surface levels of Kv1.5. More importantly Myo5bYE/QR but not Myo5bQL/YC significantly decreased channel recycling (76 ± 2.2%; n ≥ 83; $p < 0.001$) (Figure 7B, Online Figure VIIIB). As with Myo5bDN, Kv1.5-GFP accumulated in Rab11 positive perinuclear endosomes in the presence of Myo5bYE/QR (Figure 7C, Online Figure VIIIC). To further demonstrate the necessity of Rab11 coupling for MYO5B-mediated recycling of Kv1.5, we co-expressed Kv1.5-GFP together with both the constitutively active (CA) Rab11 construct and Myo5bYE/QR. Rab11-CA resulted in a significant increase in the steady-state cell surface levels of Kv1.5-GFP (29 ± 3.5%, n ≥ 74, $p < 0.001$) that was abrogated by co-expression with Myo5bYE/QR. (Figure 7D, Online Figure VIIID). Therefore, Kv1.5 channel recycling via MYO5B occurs through selective Rab11-mediated coupling to Kv1.5-contaning endosomes. These coordinate trafficking events contribute to the steady-state cell surface levels of Kv1.5 channel protein and thereby likely play a role in determining the electrical excitability of native cardiac myocytes.

DISCUSSION

We report a previously unrecognized role for MYO5A and MYO5B in the selective membrane trafficking of Kv1.5 in cardiac myocytes and elucidated the mechanism by which they act in functionally distinct steps in cell surface trafficking of Kv1.5 to selectively determine I_{Kur} current density in cardiac myocytes. The subunit specificity and functional specialization demonstrated in this study denotes a potential therapeutic avenue for the modulation of I_{Kur} in the treatment AF.

In considering channel trafficking pathways as therapeutic targets, it is important to consider that cell surface delivery of cardiovascular ion channels may occur through selective trafficking mechanisms. We show that, MYO5A and MYO5B do not play a role in determining cell surface levels of hERG, or I_{ss} current. This is somewhat surprising, given a common mechanism through the dynein motor complex for retrograde microtubule-dependent trafficking of multiple K^+ channels, including Kv1.5[54,25, 26]. However, there are distinct differences in the forward trafficking signals of channel subunits, implying a complex system for differential regulation of ER to Golgi trafficking[55]. With regard to localization, different members of the MAGUK family have been shown to interact with specific K^+ channel subunits to direct localization and regulate surface density. In particular, overexpression of SAP97 increases surface levels of Kv1.5 [31, 32, 37] and decreases other Kv channels[56], while CASK participates in the targeting of Kir2 channels[57]. Kv channel subunits also show a significant degree of specialization in their association with actin-binding proteins, for example, Kv1.5 interacts alpha-actinin-2[27, 29, 33], filamin with Kv4.2[58], and cortactin with Kv1.2[59]. Therefore, while some mechanisms of trafficking may be conserved, there are specialized steps along the pathway regulated by selective molecular motors, adaptors, and anchoring proteins. While additional channels need to be investigated to determine the full extent of selectivity of MYO5A and MYO5B for Kv1.5 channel trafficking, the data presented here further emphasize the potential for selectivity in ion channel trafficking pathways.

An intriguing result from our study is that Kv1.5 and Cx43, two proteins enriched at their respective intercalated disk regions[4, 35, 60], are both regulated by MYO5A. Microtubules are involved in delivery of Cx43 to the intercalated disc[35, 60] with actin rest stops involved in the forward trafficking pathway[36]. Selectivity for Cx43 and Kv1.5, suggests that myosin motors and actin can contribute to specificity of delivery to membrane subdomains, in particular to the intercalated disc. Future studies will help to understand how the actin and microtubule cytoskeleton interact to target channel delivery to specific cardiomyocyte subdomains.

Modulation of trafficking pathways shows promise for acute cardioversion of arrhythmias, however its role in the treatment of paroxysmal or persistent AF is less clear. AF is progressive disorder marked by electrical and structural remodeling that becomes more established with prolonged arrhythmia. Electrical remodeling is characterized by significant decreases in atrial effective refractory period, due to alterations in ion channel densities in the membrane.[14] Additionally electrical remodeling of the atria alters ion channel sensitivities to antiarrhythmic drug-mediated block[13]. This may be due in part to the marked

decrease in Kv channel surface density during AF,[14,10] reducing the functional channel available for pore block by antiarrhythmic drugs. The dependence of Kv1.5 trafficking on actin filaments demonstrated here provides insight into the correlation between electrical and structural remodeling during AF. These two pathophysiologies may be mechanistically linked through the induction of calcium-activated neutral proteases called calpains[61–63]. Activation of calpains by calcium overload may underlie the significant decrease in actin protein levels[64] and disorganization of the cytoskeletal networks observed in AF. Calpain has also been implicated in the degradation of alpha-actinin-2 during ischemia reperfusion injury[65–68]. Both disruption of the actin cytoskeleton with cytochalasin-D or antisense oligonucleotide knockdown of alpha-actinin-2 alters Kv1.5 channel current density[27, 29, 33]. Given the importance of interaction with the cytoskeleton determining the cell surface levels of Kv1.5 in myocytes, calpain activation may be one mechanism linking cytoskeletal disruption to decreases in I_{Kur} during AF. Additionally, our results predict that deterioration of the actin cytoskeleton would disrupt myosin-mediated delivery of Kv1.5 to the plasma membrane. Therefore, the ~ 50% decrease in I_{Kur} and Kv1.5 protein levels in AF may reflect a combination of decreased cell surface trafficking and enhanced endocytosis of Kv1.5 leading to channel degradation. It is unclear whether the reduction of channel levels is a compensatory response to promote survival or a maladaptive response that should be corrected. Regardless, understanding the precise mechanism regulating surface density of ion channels is an important and necessary step in considering therapeutic strategies that increase or decrease ion channels density in the myocyte membrane.

In summary, this report reveals the importance of myosin-V motors in regulating the plasma membrane targeting and cell surface density of Kv1.5 in the myocardium. This is the first report to show a role for these proteins in the trafficking and regulation of cardiovascular proteins, with a functional consequence of their disruption. As evidenced by these data, continued elucidation of the molecular machinery involved in cardiovascular protein trafficking may reveal novel therapeutic targets for the regulation and treatment of cardiovascular disease.

Supplementary Material

Refer to Web version on PubMed Central for supplementary material.

Acknowledgments

We acknowledge Kristin M. Van Genderen for technical assistance.

SOURCES OF FUNDING

This work was supported by a Systems and Integrative Biology training grant, Cardiovascular Center training grant, and Pharmaceutical Research and Manufacturers of America (PhRMA) Predoctoral Fellowship in Pharmacology/ Toxicology (S.M.S), NIH grant T32HL007853 (E.D.V), NIH grant HL094414 (R.M.S.), and NIH grant HL027093 (J.R.M.).

Nonstandard Abbreviations and Acronyms

AF	Atrial Fibrillation

BFA	Breffeldin A
CA	Constitutively Active
CASK	calcium/calmodulin-dependent serine protein kinase
Cx43	Connexin-43
DN	Dominant Negative
DPO-1	Diphenyl phosphine oxide-1
Ikur	Ultra-rapid delayed rectifier current
MAGUK	membrane-associated guanylate kinases

References

1. Amos GJ, Wettwer E, Metzger F, Li Q, Himmel HM, Ravens U. Differences between outward currents of human atrial and subepicardial ventricular myocytes. J Physiol. 1996; 491 (Pt 1):31–50. [PubMed: 9011620]
2. Camm AJ. Safety considerations in the pharmacological management of atrial fibrillation. Int J Cardiol. 2008; 127:299–306. [PubMed: 18191470]
3. Camm AJ, Savelieva I. Advances in antiarrhythmic drug treatment of atrial fibrillation: Where do we stand now? Heart Rhythm. 2004; 1:244–246. [PubMed: 15851161]
4. Mays DJ, Foose JM, Philipson LH, Tamkun MM. Localization of the kv1.5 k+ channel protein in explanted cardiac tissue. J Clin Invest. 1995; 96:282–292. [PubMed: 7615797]
5. Lafuente-Lafuente C, Mouly S, Longas-Tejero MA, Bergmann JF. Antiarrhythmics for maintaining sinus rhythm after cardioversion of atrial fibrillation. Cochrane database of systematic reviews (Online). 2007:CD005049.
6. Lafuente-Lafuente C, Mouly S, Longas-Tejero MA, Mahe I, Bergmann JF. Antiarrhythmic drugs for maintaining sinus rhythm after cardioversion of atrial fibrillation: A systematic review of randomized controlled trials. Archives of internal medicine. 2006; 166:719–728. [PubMed: 16606807]
7. Feng J, Wible B, Li GR, Wang Z, Nattel S. Antisense oligodeoxynucleotides directed against kv1.5 mrna specifically inhibit ultrarapid delayed rectifier k+ current in cultured adult human atrial myocytes. Circulation research. 1997; 80:572–579. [PubMed: 9118489]
8. Olson TM, Alekseev AE, Liu XK, Park S, Zingman LV, Bienengraeber M, Sattiraju S, Ballew JD, Jahangir A, Terzic A. Kv1.5 channelopathy due to kcna5 loss-of-function mutation causes human atrial fibrillation. Human molecular genetics. 2006; 15:2185–2191. [PubMed: 16772329]
9. Tanabe Y, Hatada K, Naito N, Aizawa Y, Chinushi M, Nawa H. Over-expression of kv1.5 in rat cardiomyocytes extremely shortens the duration of the action potential and causes rapid excitation. Biochem Biophys Res Commun. 2006; 345:1116–1121. [PubMed: 16713996]
10. Van Wagoner DR, Pond AL, McCarthy PM, Trimmer JS, Nerbonne JM. Outward k+ current densities and kv1.5 expression are reduced in chronic human atrial fibrillation. Circulation research. 1997; 80:772–781. [PubMed: 9168779]
11. Ford JW, Milnes JT. New drugs targeting the cardiac ultra-rapid delayed-rectifier current (i kur): Rationale, pharmacology and evidence for potential therapeutic value. J Cardiovasc Pharmacol. 2008; 52:105–120. [PubMed: 18670369]
12. Schumacher SM, McEwen DP, Zhang L, Arendt KL, Van Genderen KM, Martens JR. Antiarrhythmic drug-induced internalization of the atrial-specific k+ channel kv1.5. Circulation research. 2009; 104:1390–1398. [PubMed: 19443837]
13. Christ T, Wettwer E, Voigt N, Hala O, Radicke S, Matschke K, Varro A, Dobrev D, Ravens U. Pathology-specific effects of the ikur/ito/ik,ach blocker ave0118 on ion channels in human chronic atrial fibrillation. Br J Pharmacol. 2008; 154:1619–1630. [PubMed: 18536759]

14. Allessie MA, Boyden PA, Camm AJ, Kleber AG, Lab MJ, Legato MJ, Rosen MR, Schwartz PJ, Spooner PM, Van Wagoner DR, Waldo AL. Pathophysiology and prevention of atrial fibrillation. Circulation. 2001; 103:769–777. [PubMed: 11156892]
15. Ausma J, Litjens N, Lenders MH, Duimel H, Mast F, Wouters L, Ramaekers F, Allessie M, Borgers M. Time course of atrial fibrillation-induced cellular structural remodeling in atria of the goat. J Mol Cell Cardiol. 2001; 33:2083–2094. [PubMed: 11735256]
16. Thijssen VL, Ausma J, Liu GS, Allessie MA, van Eys GJ, Borgers M. Structural changes of atrial myocardium during chronic atrial fibrillation. Cardiovasc Pathol. 2000; 9:17–28. [PubMed: 10739903]
17. Goette A, Honeycutt C, Langberg JJ. Electrical remodeling in atrial fibrillation. Time course and mechanisms. Circulation. 1996; 94:2968–2974. [PubMed: 8941128]
18. Desnos C, Huet S, Darchen F. 'Should i stay or should i go?': Myosin v function in organelle trafficking. Biol Cell. 2007; 99:411–423. [PubMed: 17635110]
19. Huang JD, Brady ST, Richards BW, Stenolen D, Resau JH, Copeland NG, Jenkins NA. Direct interaction of microtubule- and actin-based transport motors. Nature. 1999; 397:267–270. [PubMed: 9930703]
20. Langford GM. Myosin-v, a versatile motor for short-range vesicle transport. Traffic. 2002; 3:859–865. [PubMed: 12453149]
21. Brown SS. Cooperation between microtubule- and actin-based motor proteins. Annu Rev Cell Dev Biol. 1999; 15:63–80. [PubMed: 10611957]
22. Hirokawa N. Kinesin and dynein superfamily proteins and the mechanism of organelle transport. Science. 1998; 279:519–526. [PubMed: 9438838]
23. Cai D, McEwen DP, Martens JR, Meyhofer E, Verhey KJ. Single molecule imaging reveals differences in microtubule track selection between kinesin motors. PLoS Biol. 2009; 7:e1000216. [PubMed: 19823565]
24. Zadeh AD, Cheng Y, Xu H, Wong N, Wang Z, Goonasekara C, Steele DF, Fedida D. Kif5b is an essential forward trafficking motor for the kv1.5 cardiac potassium channel. J Physiol. 2009; 587:4565–4574. [PubMed: 19675065]
25. Choi WS, Khurana A, Mathur R, Viswanathan V, Steele DF, Fedida D. Kv1.5 surface expression is modulated by retrograde trafficking of newly endocytosed channels by the dynein motor. Circulation research. 2005; 97:363–371. [PubMed: 16051887]
26. McEwen DP, Schumacher SM, Li Q, Benson MD, Iniguez-Lluhi JA, Van Genderen KM, Martens JR. Rab-gtpase-dependent endocytic recycling of kv1.5 in atrial myocytes. The Journal of biological chemistry. 2007; 282:29612–29620. [PubMed: 17673464]
27. Mason HS, Latten MJ, Godoy LD, Horowitz B, Kenyon JL. Modulation of kv1.5 currents by protein kinase a, tyrosine kinase, and protein tyrosine phosphatase requires an intact cytoskeleton. Mol Pharmacol. 2002; 61:285–293. [PubMed: 11809852]
28. Martens JR, Navarro-Polanco R, Coppock EA, Nishiyama A, Parshley L, Grobaski TD, Tamkun MM. Differential targeting of shaker-like potassium channels to lipid rafts. The Journal of biological chemistry. 2000; 275:7443–7446. [PubMed: 10713042]
29. Maruoka ND, Steele DF, Au BP, Dan P, Zhang X, Moore ED, Fedida D. Alpha-actinin-2 couples to cardiac kv1.5 channels, regulating current density and channel localization in hek cells. FEBS Lett. 2000; 473:188–194. [PubMed: 10812072]
30. Eldstrom J, Choi WS, Steele DF, Fedida D. Sap97 increases kv1.5 currents through an indirect n-terminal mechanism. FEBS Lett. 2003; 547:205–211. [PubMed: 12860415]
31. Eldstrom J, Doerksen KW, Steele DF, Fedida D. N-terminal pdz-binding domain in kv1 potassium channels. FEBS Lett. 2002; 531:529–537. [PubMed: 12435606]
32. Murata M, Buckett PD, Zhou J, Brunner M, Folco E, Koren G. Sap97 interacts with kv1.5 in heterologous expression systems. Am J Physiol Heart Circ Physiol. 2001; 281:H2575–2584. [PubMed: 11709425]
33. Cukovic D, Lu GW, Wible B, Steele DF, Fedida D. A discrete amino terminal domain of kv1.5 and kv1.4 potassium channels interacts with the spectrin repeats of alpha-actinin-2. FEBS Lett. 2001; 498:87–92. [PubMed: 11389904]

34. Cheng L, Yung A, Covarrubias M, Radice GL. Cortactin is required for n-cadherin regulation of kv1.5 channel function. The Journal of biological chemistry. 2011; 286:20478–20489. [PubMed: 21507952]
35. Smyth JW, Hong TT, Gao D, Vogan JM, Jensen BC, Fong TS, Simpson PC, Stainier DY, Chi NC, Shaw RM. Limited forward trafficking of connexin 43 reduces cell-cell coupling in stressed human and mouse myocardium. J Clin Invest. 2010; 120:266–279. [PubMed: 20038810]
36. Smyth JW, Vogan JM, Buch PJ, Zhang SS, Fong TS, Hong TT, Shaw RM. Actin cytoskeleton rest stops regulate anterograde traffic of connexin 43 vesicles to the plasma membrane. Circulation research. 2012; 110:978–989. [PubMed: 22328533]
37. Abi-Char J, El-Haou S, Balse E, Neyroud N, Vranckx R, Coulombe A, Hatem SN. The anchoring protein sap97 retains kv1.5 channels in the plasma membrane of cardiac myocytes. Am J Physiol Heart Circ Physiol. 2008; 294:H1851–1861. [PubMed: 18245566]
38. Dantzig JA, Liu TY, Goldman YE. Functional studies of individual myosin molecules. Ann N Y Acad Sci. 2006; 1080:1–18. [PubMed: 17132771]
39. Zhao LP, Koslovsky JS, Reinhard J, Bahler M, Witt AE, Provance DW Jr, Mercer JA. Cloning and characterization of myr 6, an unconventional myosin of the dilute/myosin-v family. Proc Natl Acad Sci U S A. 1996; 93:10826–10831. [PubMed: 8855265]
40. Thibodeau IL, Xu J, Li Q, Liu G, Lam K, Veinot JP, Birnie DH, Jones DL, Krahn AD, Lemery R, Nicholson BJ, Gollob MH. Paradigm of genetic mosaicism and lone atrial fibrillation: Physiological characterization of a connexin 43-deletion mutant identified from atrial tissue. Circulation. 2010; 122:236–244. [PubMed: 20606116]
41. Smyth JW, Shaw RM. Autoregulation of connexin43 gap junction formation by internally translated isoforms. Cell Rep. 2013; 5:611–618. [PubMed: 24210816]
42. Pierobon P, Achouri S, Courty S, Dunn AR, Spudich JA, Dahan M, Cappello G. Velocity, processivity, and individual steps of single myosin v molecules in live cells. Biophys J. 2009; 96:4268–4275. [PubMed: 19450497]
43. Yildiz A, Forkey JN, McKinney SA, Ha T, Goldman YE, Selvin PR. Myosin v walks hand-overhand: Single fluorophore imaging with 1.5-nm localization. Science. 2003; 300:2061–2065. [PubMed: 12791999]
44. Mehta AD, Rock RS, Rief M, Spudich JA, Mooseker MS, Cheney RE. Myosin-v is a processive actin-based motor. Nature. 1999; 400:590–593. [PubMed: 10448864]
45. Vale RD, Milligan RA. The way things move: Looking under the hood of molecular motor proteins. Science. 2000; 288:88–95. [PubMed: 10753125]
46. Baker JE, Krementsova EB, Kennedy GG, Armstrong A, Trybus KM, Warshaw DM. Myosin v processivity: Multiple kinetic pathways for head-to-head coordination. Proc Natl Acad Sci U S A. 2004; 101:5542–5546. [PubMed: 15056760]
47. Song BD, Leonard M, Schmid SL. Dynamin gtpase domain mutants that differentially affect gtp binding, gtp hydrolysis, and clathrin-mediated endocytosis. The Journal of biological chemistry. 2004; 279:40431–40436. [PubMed: 15262989]
48. Ullrich O, Reinsch S, Urbe S, Zerial M, Parton RG. Rab11 regulates recycling through the pericentriolar recycling endosome. The Journal of cell biology. 1996; 135:913–924. [PubMed: 8922376]
49. Ren M, Xu G, Zeng J, De Lemos-Chiarandini C, Adesnik M, Sabatini DD. Hydrolysis of gtp on rab11 is required for the direct delivery of transferrin from the pericentriolar recycling compartment to the cell surface but not from sorting endosomes. Proc Natl Acad Sci U S A. 1998; 95:6187–6192. [PubMed: 9600939]
50. Swiatecka-Urban A, Talebian L, Kanno E, Moreau-Marquis S, Coutermarsh B, Hansen K, Karlson KH, Barnaby R, Cheney RE, Langford GM, Fukuda M, Stanton BA. Myosin vb is required for trafficking of the cystic fibrosis transmembrane conductance regulator in rab11a-specific apical recycling endosomes in polarized human airway epithelial cells. The Journal of biological chemistry. 2007; 282:23725–23736. [PubMed: 17462998]
51. Treharne KJ, Crawford RM, Mehta A. Cftr, chloride concentration and cell volume: Could mammalian protein histidine phosphorylation play a latent role? Exp Physiol. 2006; 91:131–139. [PubMed: 16219660]

52. Wang Z, Edwards JG, Riley N, Provance DW Jr, Karcher R, Li XD, Davison IG, Ikebe M, Mercer JA, Kauer JA, Ehlers MD. Myosin vb mobilizes recycling endosomes and ampa receptors for postsynaptic plasticity. Cell. 2008; 135:535–548. [PubMed: 18984164]

53. Roland JT, Bryant DM, Datta A, Itzen A, Mostov KE, Goldenring JR. Rab gtpase-myo5b complexes control membrane recycling and epithelial polarization. Proc Natl Acad Sci U S A. 2011; 108:2789–2794. [PubMed: 21282656]

54. Loewen ME, Wang Z, Eldstrom J, Dehghani Zadeh A, Khurana A, Steele DF, Fedida D. Shared requirement for dynein function and intact microtubule cytoskeleton for normal surface expression of cardiac potassium channels. Am J Physiol Heart Circ Physiol. 2009; 296:H71–83. [PubMed: 18978193]

55. Steele DF, Eldstrom J, Fedida D. Mechanisms of cardiac potassium channel trafficking. J Physiol. 2007; 582:17–26. [PubMed: 17412767]

56. Tiffany AM, Manganas LN, Kim E, Hsueh YP, Sheng M, Trimmer JS. Psd-95 and sap97 exhibit distinct mechanisms for regulating k(+) channel surface expression and clustering. The Journal of cell biology. 2000; 148:147–158. [PubMed: 10629225]

57. Leonoudakis D, Conti LR, Radeke CM, McGuire LM, Vandenberg CA. A multiprotein trafficking complex composed of sap97, cask, veli, and mint1 is associated with inward rectifier kir2 potassium channels. The Journal of biological chemistry. 2004; 279:19051–19063. [PubMed: 14960569]

58. Petrecca K, Miller DM, Shrier A. Localization and enhanced current density of the kv4.2 potassium channel by interaction with the actin-binding protein filamin. J Neurosci. 2000; 20:8736–8744. [PubMed: 11102480]

59. Hattan D, Nesti E, Cachero TG, Morielli AD. Tyrosine phosphorylation of kv1.2 modulates its interaction with the actin-binding protein cortactin. The Journal of biological chemistry. 2002; 277:38596–38606. [PubMed: 12151401]

60. Shaw RM, Fay AJ, Puthenveedu MA, von Zastrow M, Jan YN, Jan LY. Microtubule plus-end-tracking proteins target gap junctions directly from the cell interior to adherens junctions. Cell. 2007; 128:547–560. [PubMed: 17289573]

61. Brundel BJ, Henning RH, Kampinga HH, Van Gelder IC, Crijns HJ. Molecular mechanisms of remodeling in human atrial fibrillation. Cardiovasc Res. 2002; 54:315–324. [PubMed: 12062337]

62. Brundel BJ, Ausma J, van Gelder IC, Van der Want JJ, van Gilst WH, Crijns HJ, Henning RH. Activation of proteolysis by calpains and structural changes in human paroxysmal and persistent atrial fibrillation. Cardiovasc Res. 2002; 54:380–389. [PubMed: 12062342]

63. Brundel BJ, Kampinga HH, Henning RH. Calpain inhibition prevents pacing-induced cellular remodeling in a hl-1 myocyte model for atrial fibrillation. Cardiovasc Res. 2004; 62:521–528. [PubMed: 15158144]

64. Schafler AE, Friedl R, Hekmat K, Hannekum A, Kirmanoglou K. Chronic atrial fibrillation: Decreased actin expression in patients with chronic atrial fibrillation. J Cardiovasc Surg (Torino). 2008; 49:83–86.

65. Van Eyk JE, Powers F, Law W, Larue C, Hodges RS, Solaro RJ. Breakdown and release of myofilament proteins during ischemia and ischemia/reperfusion in rat hearts: Identification of degradation products and effects on the pca-force relation. Circulation research. 1998; 82:261–271. [PubMed: 9468197]

66. Matsumura Y, Saeki E, Inoue M, Hori M, Kamada T, Kusuoka H. Inhomogeneous disappearance of myofilament-related cytoskeletal proteins in stunned myocardium of guinea pig. Circulation research. 1996; 79:447–454. [PubMed: 8781478]

67. Goll DE, Dayton WR, Singh I, Robson RM. Studies of the alpha-actinin/actin interaction in the z-disk by using calpain. The Journal of biological chemistry. 1991; 266:8501–8510. [PubMed: 2022664]

68. Barta J, Toth A, Edes I, Vaszily M, Papp JG, Varro A, Papp Z. Calpain-1-sensitive myofibrillar proteins of the human myocardium. Mol Cell Biochem. 2005; 278:1–8. [PubMed: 16180082]

Novelty and Significance

What Is Known?

- Atrial fibrillation is one of the most common cardiac arrhythmias.
- Current pharmacology exhibits a significant risk for proarrhythmia in the ventricles due to an overlap in the target ion channels.
- New therapeutic strategies focus on atrial selective proteins and regulatory mechanisms.

What New Information Does This Article Contribute?

- There is selectivity in the motor proteins utilized for trafficking of ion channels in the heart.
- This selectivity may represent novel targets for the treatment of atrial fibrillation.

At present, long-term therapy for atrial fibrillation poses a significant risk to ventricular function due to a lack of drug selectivity. Therefore, there remains a need for ventricular sparing treatments that would be safe and effective for clinical use. An uninvestigated realm for atrial selective treatment is the regulatory and selective trafficking steps for ion channels in the heart. This study demonstrates, for the first time, that there is specificity in the motor proteins utilized for ion channel surface trafficking in the heart. These motor proteins demonstrate selectivity in regulating distinct steps in the trafficking of a particular ion channel to the plasma membrane. This study elucidates a component of the trafficking machinery in the heart and reveals that all membrane delivery does not occur through a common mechanism. This is distinct from the current focus on drugs that block ion channels, for which a significant degree of overlap has been observed. Importantly, the discovery of such channel specific trafficking pathways may lead to the development of novel therapeutics for long-term maintenance of atrial rhythm and treatment of other cardiovascular arrhythmias.

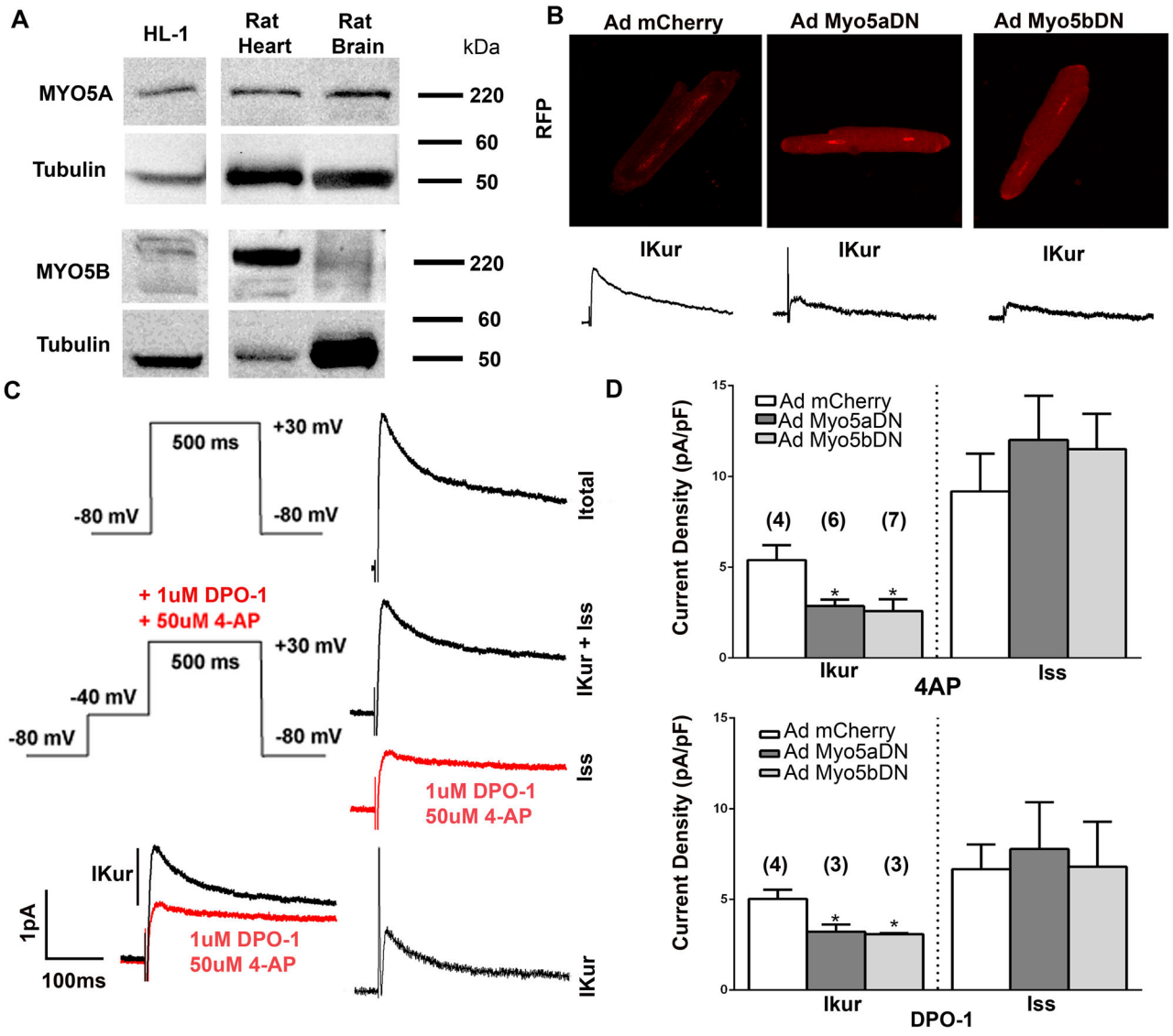

Figure 1. Endogenous MYO5A and MYO5B regulate I_{Kur}

(A) Representative western blot images of endogenous MYO5A, MYO5B and tubulin from non-transfected HL1 cells and rat heart and brain. **(B)** Representative images of ventricular myocytes demonstrating fluorescence 24 hr post transduction with mCherry, MYO5aDN or Myo5bDN. **(C)** Representative traces of voltage protocol, pharmacological steps, and electronic subtraction for isolation of I_{Kur} current in acutely dissociated myocytes. **(D)** Quantification of I_{Kur} and I_{ss} current, and representative traces of I_{Kur} current, in acutely dissociated myocytes 24 hr post transduction ($n \geq 7$ myocytes). *$p < 0.05$; **$p < 0.01$ by one-way ANOVA with Tukey post-test.

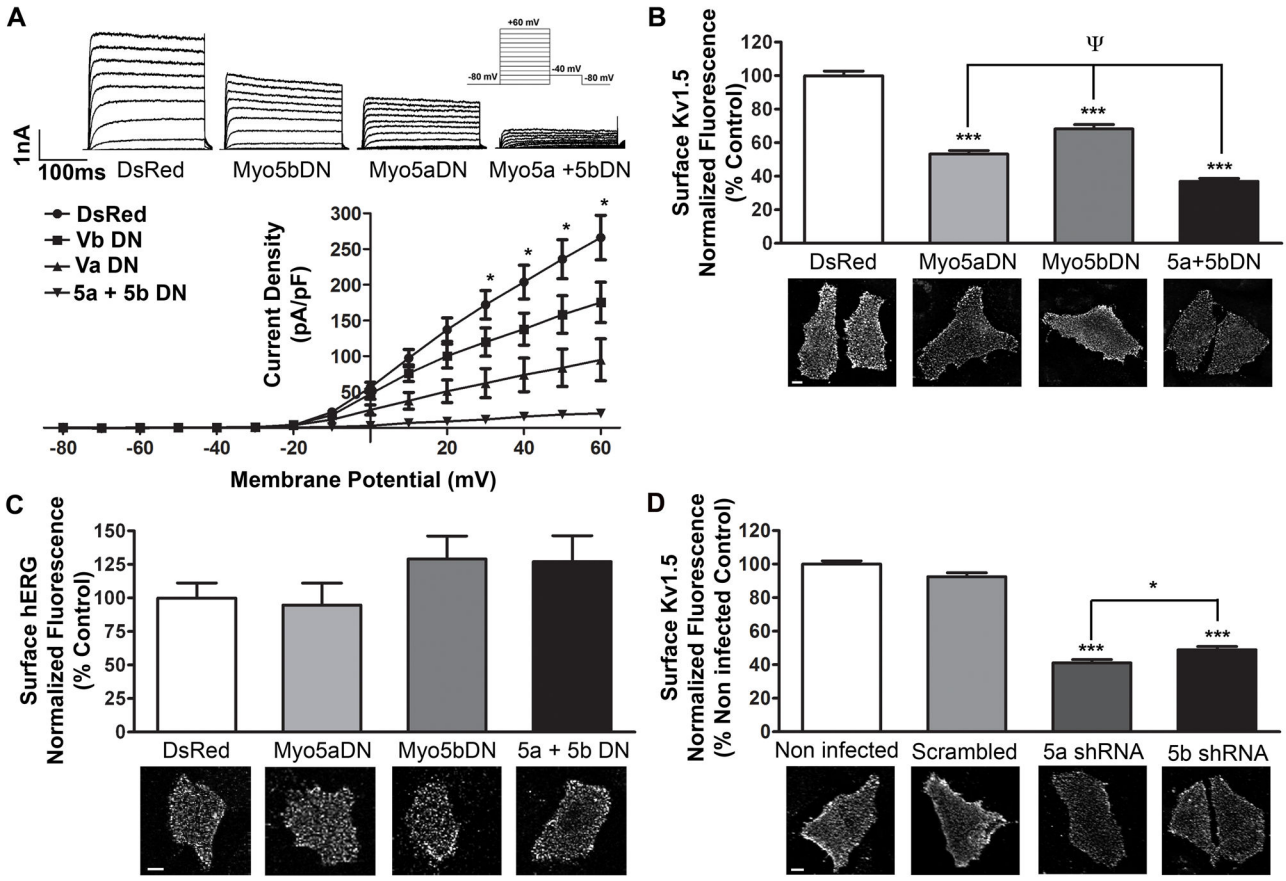

Figure 2. Disruption of MYO5A and MYO5B function decreases current density and cell surface levels of Kv1.5

HL-1 cells transfected with Kv1.5-GFP or hERG-GFP, and co-expressing either DsRed vector control, Myo5aDN or Myo5bDN alone or in combination. **(A)** Representative whole cell voltage clamp current traces and the corresponding IV curve for Kv1.5 current density. **(B)** Quantification of surface Kv1.5-GFP with representative images for each condition. **(C)** Quantification of surface hERG-GFP with representative images for each condition. **(D)** Quantification of surface Kv1.5-GFP with representative images following 48 hr of lentiviral infection with scrambled, Myo5A, or Myo5b shRNA. Scale bars = 10μm. *$p < 0.05$; ***$p < 0.001$ by one-way ANOVA with Tukey post-test.

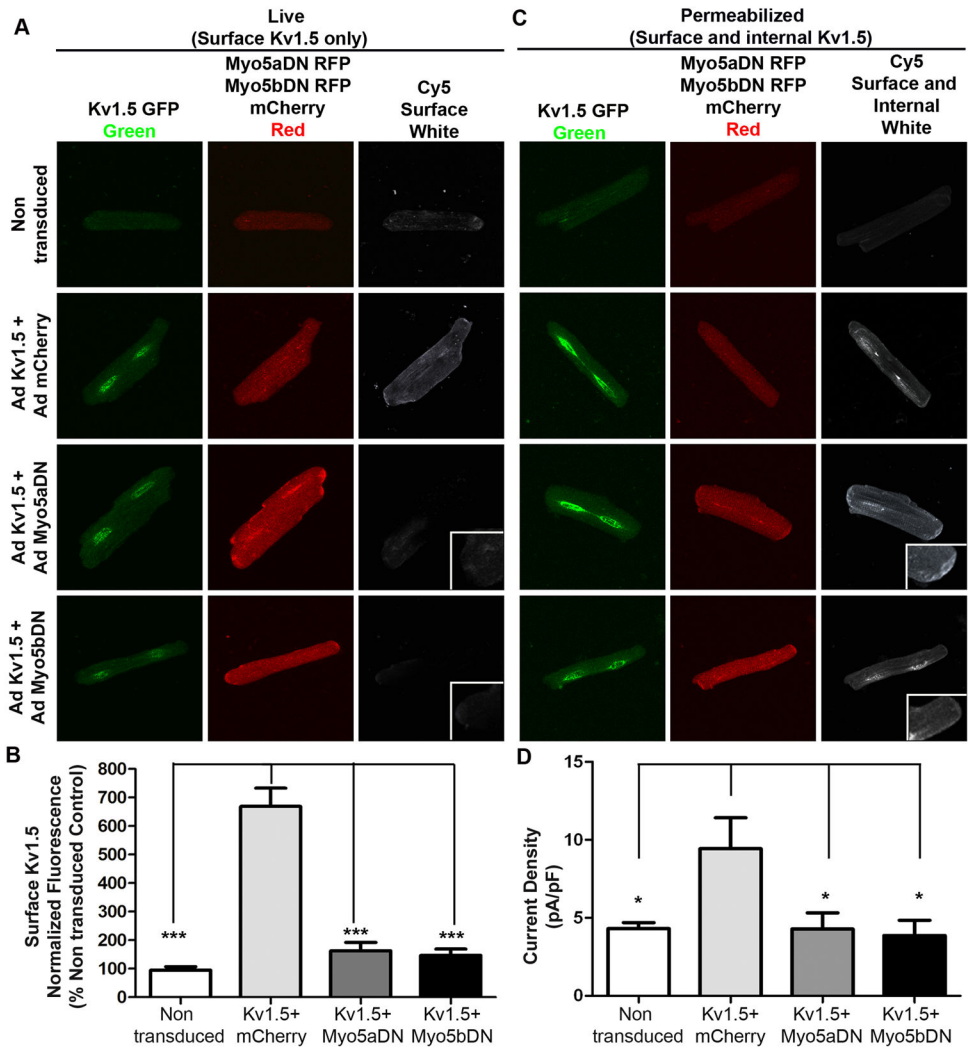

Figure 3. Disruption of MYO5A and MYO5B function decreases current density and cell surface levels of Kv1.5 and increases accumulation at cell-cell borders

Adult rat ventricular myocytes co-transduced with Kv1.5-GFP and either mCherry, Myo5aDN, or Myo5bDN and analyzed 24hrs later. **(A)** Representative images of live cell imaging. **(B)** Quantification of images of steady-state surface Kv1.5-GFP levels under each condition. **(C)** Representative images of fixed and permeabilized cells. **(D)** Quantification of I_{Kur} current density. * $p < 0.05$; *** $p < 0.001$, by one-way ANOVA with Tukey post-test.

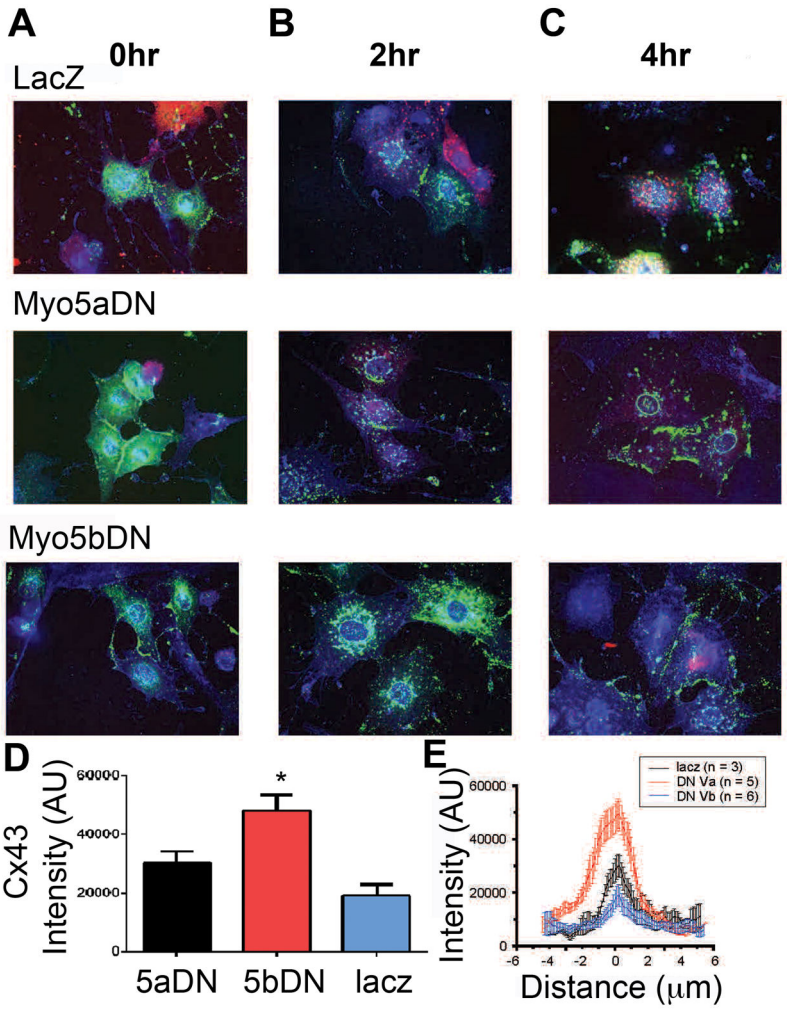

Figure 4.

MYO5A is necessary for anterograde movement of connexin-43 (Cx43) from the ER/golgi apparatus to the plasma membrane in neonatal ventricular cardiomyocytes. **(A)** Representative images of cells co-transduced with Cx43 (green) and either LacZ, MYO5aDN, or Myo5bDN constructs (red), (n=3, 4, and 6 respectively), followed by a 12 hour treatment with Brefeldin A (BFA), to inhibit the anterograde movement of proteins from the ER/Golgi region to the plasma membrane, including 2 and 4 hour post BFA washout. **(B** and **C)** Fluorescence intensity profile for Cx43 at the cell-cell border. *$p < 0.05$, by one-way ANOVA with Tukey post-test.

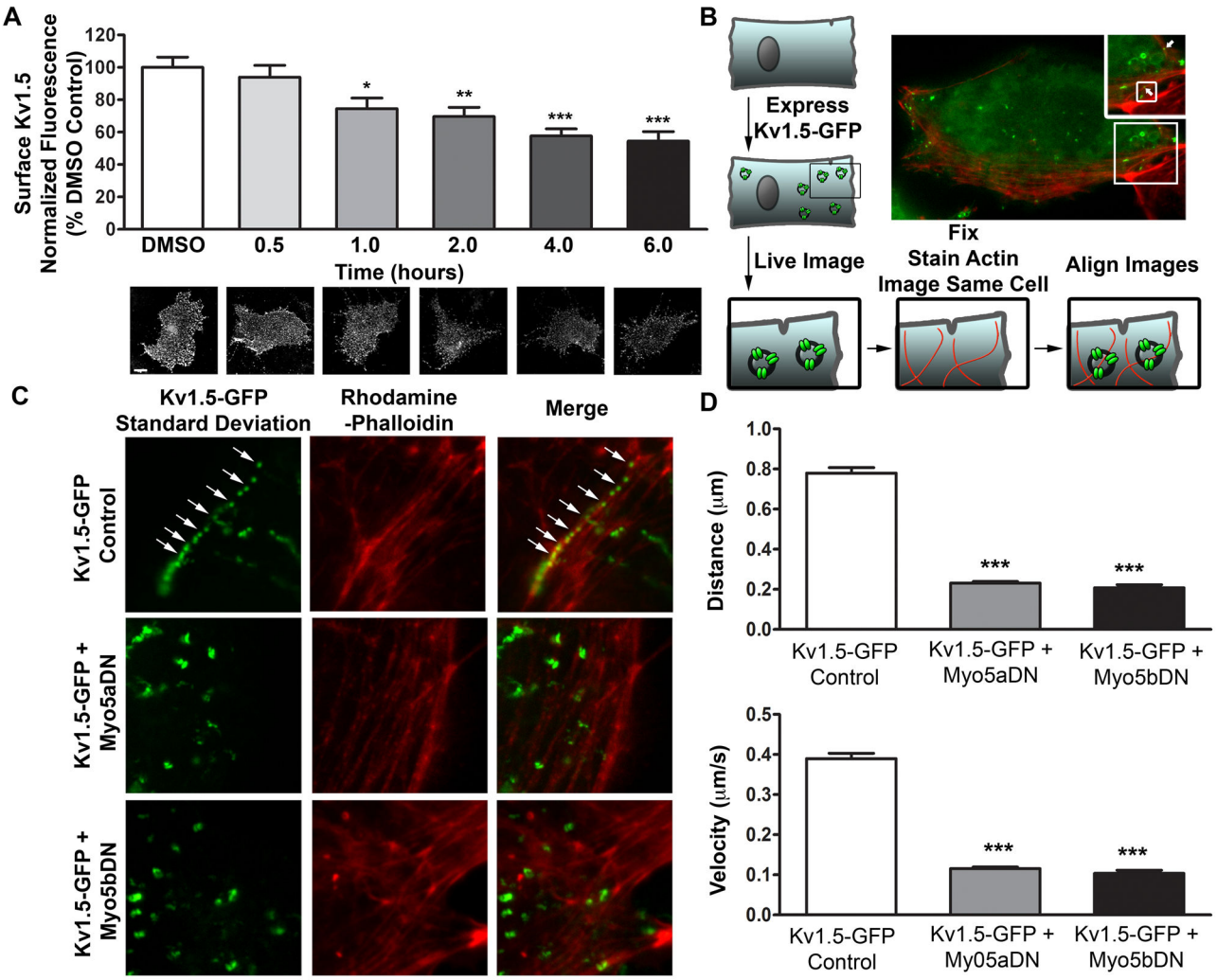

Figure 5. Processivity of Kv1.5-containing vesicles is lost upon inhibition of MYO5A and MYO5B

(A) Quantification of surface channel and representative images for HL-1 cells 48 hr post transfection with Kv1.5-GFP. Cells were treated with 0.1% DMSO vehicle control or 5 μmol/L cytochalasin D for 0.5, 1, 2, 4, and 6 hr. **(B)** Representation of the protocol for live cell imaging, and representative image, of Kv1.5-GFP+ vesicle trafficking and retrospective actin filament labeling. **(C)** Representative images showing the SD map for Kv1.5-GFP+ vesicle motility, rhodamine phalloidin fluorescence, and the merged image. **(D)** Quantification of the distance traveled and velocity of Kv1.5-GFP+ vesicles trafficking along actin filaments in the periphery of the cell (n = 20 tracks from 16 cells, 17 tracks from 4 cells, and 9 tracks from 2 cells for Kv1.5 alone, Kv1.5 + myosin Va DN, and Kv1.5 + myosin Vb DN, respectively). Scale bars = 10μm. * $p < 0.05$; ** $p < 0.01$; *** $p < 0.001$ by one-way ANOVA with Tukey post-test.

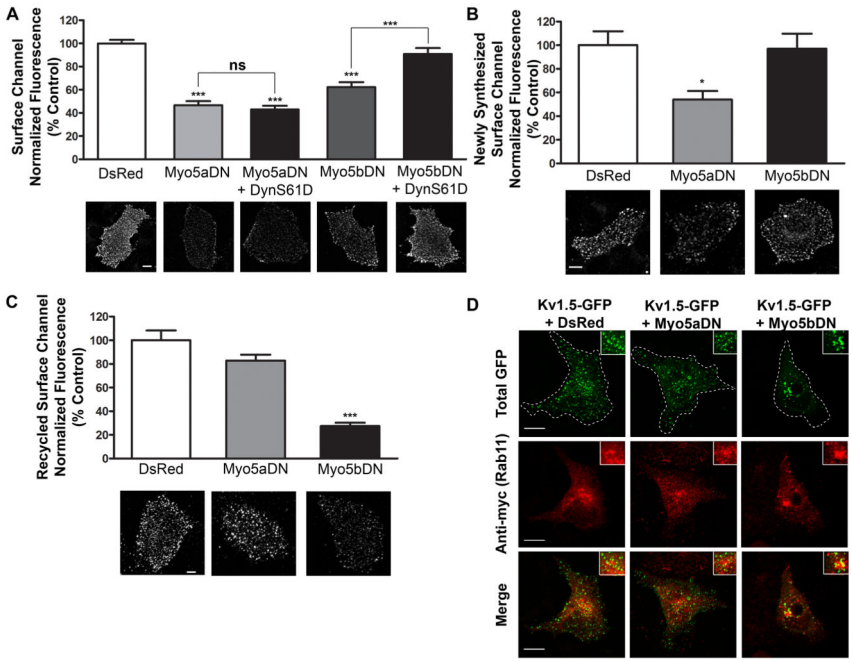

Figure 6. MYO5A acts in the anterograde trafficking, and MYO5B in the post-endocytic recycling of Kv1.5

HL-1 cells transiently expressing Kv1.5-GFP 48 hr post transfection. **(A)** Quantification and representative images of steady-state surface expression of Kv1.5 upon co-expression with DsRed, MYO5aDN, MYO5aDN + dynS61D, Myo5bDN, or Myo5bDN + dynS61D. **(B)** Quantification and representative images of newly synthesized Kv1.5-GFP at the surface 6 hr post expression. **(C)** Quantification and representative images of Kv1.5-GFP recycled to the surface. **(D)** Co-localization for Kv1.5-GFP, Rab11, and MYO5aDN or Myo5bDN in perinuclear endosomes. Scale bars = 10μm. * $p < 0.05$; *** $p < 0.001$ by one-way ANOVA with Tukey post-test.

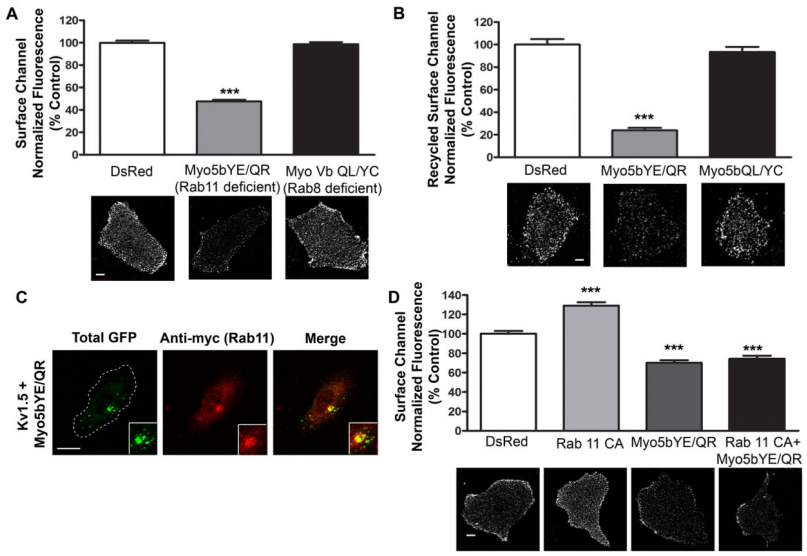

Figure 7. Recycling of Kv1.5 requires selective interaction of MYO5B with Rab11

Quantification and representative images of HL-1 cells transiently expressing Kv1.5-GFP 48 hr post transfection. **(A)** Steady-state surface expression of Kv1.5-GFP in the presence of Myo5bYE/QR or Myo5bQL/YC. **(B)** Quantification and images of Kv1.5-GFP recycled to the surface. **(C)** Co-localization for Kv1.5-GFP, Rab11, and Myo5bYE/QR in perinuclear endosomes. **(D)** Steady-state surface Kv1.5 upon co-expression with Rab11-CA, Myo5bYE/QR, or Rab11-CA and Myo5bYE/QR. Scale bars = 10μm. *** $p < 0.001$ by one-way ANOVA with Tukey post-test.

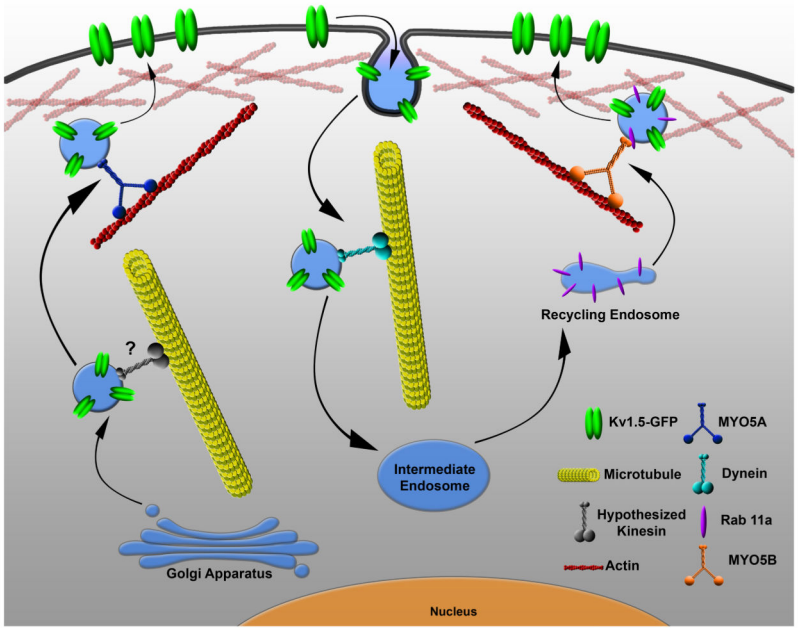

Figure 8.
Proposed model for Kv1.5 trafficking in myocytes.